Design, implementation, and metrological characterization of a wearable, integrated AR-BCI hands-free system for health 4.0 monitoring

Measurement (2021)

Contents lists available at ScienceDirect

Measurement

journal homepage: www.elsevier.com/locate/measurement

Design, implementation, and metrological characterization of a wearable, integrated AR-BCI hands-free system for health 4.0 monitoring

Pasquale Arpaia[a,b], Egidio De Benedetto[a,*], Luigi Duraccio[a,c]

[a] University of Naples Federico II - Department of Information Technology and Electrical Engineering, Naples, Italy
[b] University of Naples Federico II - Interdepartmental Research Center in Health Management and Innovation in Healthcare (CIRMIS), Naples, Italy
[c] Polytechnic University of Turin - Department of Electronics and Telecommunications, Turin, Italy

ARTICLE INFO

Article history:
Received X Month 2020

Keywords:
Augmented reality
Brain-Computer Interface
SSVEP
Digital transformation
Medical instruments
Health 4.0
Healthcare
Monitoring Systems
Patient's vitals
Wearable

ABSTRACT

An integrated real-time monitoring system based on Augmented Reality (AR) and Brain-Computer Interface (BCI) for hands-free acquisition and visualization of remote data is proposed. As a case study, the monitoring of patients' vitals in the operating room (OR) is considered; in particular, through the suitable combination of BCI and AR, the anesthetist can monitor in real-time (through a set of AR glasses), the patient's vitals acquired from the electromedical equipment. Healthcare-related applications are particularly demanding in terms of real-time requirements; hence, the considered scenario represents an interesting and challenging testbed for the proposed system. Experimental tests were carried out at the University Hospital Federico II (Naples, Italy), employing pieces of equipment that are generally available in the OR. After the preliminary functional validation, accuracy and delay were measured, demonstrating the effectiveness and reliability of the proposed AR-BCI-based monitoring system.

1. Introduction

The use of the 4.0 enabling technologies is rapidly extending also to other application contexts, such as finance, agriculture, public administration, constructions, and healthcare [1, 2]. In particular, information technologies such as the Internet of Things [3]; brain-computer interface (BCI) [4, 5]; artificial intelligence [6, 7]; machine learning [8]; cloud computing [9]; additive manufacturing [10]; wearable sensors [11–14]; as well as augmented, virtual, and mixed realities (AR, VR, & MR) [15, 16] are fostering the digital transformation in healthcare. These technologies represent the pillars of medical cyber-physical systems, which represent the most notable expression of the 4.0 Era, able to provide a more effective service and environment of healthcare [17–19]. Indeed, the health 4.0 paradigm is leaning towards a user-centered approach, with the aim to guarantee a flawless and natural interaction of the user with the technological systems, also resorting to novel computer/human interfaces such as BCI and AR.

BCIs can interpret human intentions through the analysis of the user's neuronal activity. BCIs can be considered as a powerful system to communicate with the external world [20], capable to create a direct link between man and computer. Originally, BCIs were mostly used as a communication means to support people with neurological disabilities [21]. However, in the last decade, the adoption of BCI has extended also to new application fields [22], such as gaming, entertainment, education, or robotics [23–26].

With regard to augmented reality, this technology overlays digitally-created content (often, in the form of images or text)

*Corresponding author: Tel.: +39-081-7683163;
e-mail: egidio.debenedetto@unina.it (Egidio De Benedetto)

to the surrounding reality, thus *augmenting* the user's perception of reality. Healthcare is benefiting from the technological growth of AR, as this is being investigated for a number of medical applications, such as preoperative surgical planning and image guided surgery [27–31]. AR is also employed to display on a set of wearable smart glasses the information related to the patient's health (e.g., the electronic medical records or the patient's vitals acquired from the medical instrumentation). For example, during surgical procedures, the anesthetist can access the patient's information directly through the AR glasses, without having to turn around and look at instrumentation [32–34]. The adoption of AR glasses, in fact, can reduce by more than one third the number of times the operator has to shift attention from the patient to the equipment; as a result, the operator can intervene promptly in case of alert.

The suitable integration of AR with BCIs represents a promising solution to achieve and improve a hands-free, human-machine interaction [35]. Recent works, related to Industry 4.0 worker stress monitoring, and ADHD/ASD children rehabilitations [5, 36–38] have managed to overcome cost and wearability issues [39], using off-the-shelf components and single-channel systems. However, so far, the combination of AR and BCI has not been addressed in a very critical application context, such as the medical one. Healthcare-related applications are particularly demanding in terms of real-time requirements; hence, the considered scenario represents an interesting test-bed for the proposed AR-BCI system.
The typical requirements for AR applications include display resolution, field of view, rendering capability, connectivity, wearability, and latency [40]. In particular, latency is one of the most critical: in fact, real-time applications generally require maximum delays in the order of 75 ms for online gaming and 250 ms [41, 42] for telemetry, to prevent phenomenona such as motion sickness. In the literature, a clinical assessment of a real-time wireless transmission was carried out in [43], where the transmission bandwidth, the number and the duration of the stops, and the monitoring delay were analyzed to assess the quality of the transmission. Also, in [44], the main challenges related to mobile healthcare applications were explored, dealing with latency, reliability, bandwidth, energy efficiency, and security. Results reported in [44] indicate that, to guarantee a proper interaction between the user and the system, video/audio delay should not exceed 300 ms.

On the basis of the aforementioned considerations, the case study considered in this work is a typical scenario during surgical procedures, where the anesthetist has to monitor in real-time the patient's vitals. In such a context, a wearable BCI-AR system for real-time monitoring of patient's vitals is proposed and experimentally characterized. More specifically, a wearable, differential single-channel BCI based on *Steady State Visually Evoked Potentials* (SSVEPs) is presented, wherein AR smart glasses are used for the generation of the flickering stimuli and for displaying the patient's vital parameters coming from the medical equipment. Dry, noninvasive electrodes are used, together with off-the-shelf components, to acquire and process the Electroencephalographic (EEG) signal. With respect to recent literature [5, 36, 45], in this work, also the possibility of using four flickering stimuli instead of two is investigated, while preserving the single-channel configuration and at the same time, aiming to keep the current performance.

The present paper is organized as follows. Section 2 summarizes provides an overview of the theoretical background of BCI. In Section 3, the proposed monitoring system is described in detail, focusing both on the overall architecture and on the integration of AR and BCI. Section 4 addresses the implementation of the system: particular attention is dedicated to the AR-BCI hardware and to the communication between the devices. Section 5 presents the performance analysis of the implemented AR-BCI integrated system. Section 6 describes the experimental setup, the function validation and the metrological characterization of the monitoring system. Finally, in Section 7, conclusions are drawn.

2. BCI theoretical background

Brain signals can be captured by means of functional magnetic resonance (fMRI), magnetoencephalography (MEG), or near-infrared spectroscopy (NIRS). However, EEG is considered as the best choice for its non-invasiveness, time-response, high accuracy, usability and low cost [20, 46]. The most used BCI paradigms are (i) P300; (ii) SSVEPs; (iii) event-related potentials (ERPs); and (iv) sensorimotor rhythms (SMR).
In particular, SSVEPs and ERPs (event-related potentials) are potentials triggered by an event.
However, ERPs are endogenous [47] potentials: ERPs are triggered by the mental act of the subject; hence, they have higher latency as they involve stronger mental processes. For example, P300 is an ERP potential occurring 300 ms after a stimulus, and it is largely used in BCI speller application [48]. Sensorimotor rhythm are related to variations of power in the band 8-25 Hz, generated by the execution or the imagination of a movement of a part of the body [49].
On the other hand, SSVEPs are exogenous potentials [50], since the response is physiological and can be measured even after less than 100 ms. Compared to the aforementioned ERP signals, SSVEPs have a fixed frequency oscillation that allows easier detection, even when using fewer electrodes, or in more noisy conditions. SSVEPs [51–53] represent a promising choice for practical applications, as they achieve high levels of accuracy and reproducibility [51, 54, 55] without the need of training for the user [45, 56]. Additionally, the BCI-SSVEP paradigm guarantees an optimal trade-off between wearability and performance, ensuring low response times.
SSVEPs are induced in the primary visual cortex when observing intermittent visual stimuli [57]. For most of the subjects, a majority of signal energy lies within the band 8-15 Hz [51]. SSVEP signals have the same periodicity of the external stimuli and have been used in many applications in the last decade, from home appliances control to spelling systems, video-games, robots, quadcopters and prosthesis control [45, 58–62].
Extracting meaningful information from noisy SSVEP signals in reasonable time and with high precision (while preserving user comfort), is a major challenge: the main difficulties arise

from the type of electrodes, which often require the application of specific solutions to improve the quality of the contact and, therefore, the signal-to-noise ratio (SNR). The number of electrodes also contributes to signal identification, where the combined information increases the SNR, especially at short intervals. In [63], for example, a robotic arm has been controlled using a 10-channels SSVEP-based BCI reaching an accuracy of 92.78% and 4 s response time.

Different studies investigated the effects of stimuli properties on the brain response [64, 65]. In particular, it has been observed that SSVEP power increases considerably with increasing contrast and decreasing distance of the user from the visual stimuli. Moreover, the number of simultaneous stimuli and their inter-distance affect both the user's attention and the brain response. Hence, VR head-mounted display and AR glasses are optimal candidates for generating visual stimuli, since the images of the flickering stimuli can be projected straight towards the eyes, thus reducing the noise factors of the surrounding environment.

3. Proposal

3.1. Basic ideas

As aforementioned, the present work proposes an integrated BCI-AR system, in which AR glasses are used 1) to monitor the patient's vitals acquired in real time from the medical instrumentation, and 2) to render the visual stimuli for the BCI-SSVEP system. The brain-driven selection is used to navigate the AR menu, showing the patient's vital signs in real-time.
The proposed BCI-AR system operates as follows. The user wears the AR glasses and the EEG electrodes; the system receives the patient's vitals from the operating room equipment, and displays them in real time on the AR glasses. Through a BCI, the user can select which parameters they want to be displayed. In the following section, the conceptual architecture and his described in detail.

3.2. Architecture

As shown in Fig. 1, the general architecture of the proposed system includes three major blocks:

- The *Monitoring Equipment*;
- The *Equipment Control Unit (ECU)*; and
- The *AR-BCI Integrated System*.

The expression *Monitoring Equipment* is used to indicate a generic set of measuring instruments, whose output data can be monitored in real time through the AR-BCI integrated system.

The *AR-BCI* subsystem allows the user to select which information, acquired from the *Monitoring Equipment*, he/she would like to be displayed in AR. More specifically, the *AR Glasses* render the flickering visual stimuli that are used to elicit the SSVEP in the user's brain. Each flickering visual stimulus is associated to one possible user's selection.
Then, the *EEG Wearable Transducer* (which includes the *Electrodes* and an *Acquisition Unit*), acquires and digitizes the EEG signal. This signal is elaborated by the *Processing Unit*, and the result is sent by the *Wireless Transceiver* to the *ECU*.

The *ECU* collects the data from the *Monitoring Equipment*. Once the data are received by the *Data Collector* unit, the *ECU* sends the output data (as selected by the user through the BCI) to display on the *AR Glasses*. This communication occurs by means of the *Wireless Transceiver*.
The *ECU* is also equipped with a *Measurement System*, which can assess the performance of the system. In particular, the quality of the transmission is assessed, expressed in terms of accuracy and latency for both data update and communication delay.
Finally, a *Metrological Characterization* feature is also included in the *ECU*, to report the results related to the quality of the transmission.

3.3. AR-BCI Integrated System

The *AR-BCI Integrated System* (Fig. 2) allows (i) the rendering of the visual stimuli for BCI-SSVEP, and (ii) the visualization in real time of the acquired parameters.
The highly-wearable BCI equipment includes EEG active dry *Electrodes* to acquire the EEG signal from the user scalp, and an *Acquisition Unit* to digitize the signal.
This BCI equipment, integrated with the AR Glasses, allows to select which data output to display among those available from the *Monitoring Equipment*. The result of the processing is sent by the *Wireless Transceiver* to the *ECU*, which collects the data from the instrumentation and sends them wirelessly to the AR Glasses, according to the user's selection.
Overall, the *AR/BCI platform* includes:

- A *Processing Unit* to detect the observed stimulus;
- The *AR glasses* which provide the visual stimuli for the BCI and also the visual feedback; and
- The *Wireless Transceiver* for the communication.

3.3.1. EEG wearable transducer

The *AR Glasses* are used to generate the visual stimuli to elicit SSVEP response in the user's EEG [51]. Then, three electrodes, placed on the user scalp, are used to acquire the EEG signal in a single-channel differential measurement. As can be seen from Fig. 2, according to International 10-20 System [5, 36], brain signals are captured using two active electrodes positioned at the Frontal Midline (Fz) and Occipital Midline (Oz) positions, connected to the negative and positive input of the acquisition unit, respectively. A passive electrode, DRL (Driven Right Leg), is positioned on the earlobe and acts as a reference. The Fz and DRL electrodes contacts are gold-plated, flat surfaces, while the Oz electrode was modified by adding eight gold-plated spring connectors, to ensure a more effective skin contact through the hair. Signals acquired through the electrodes are digitized by the *Acquisition Unit*.

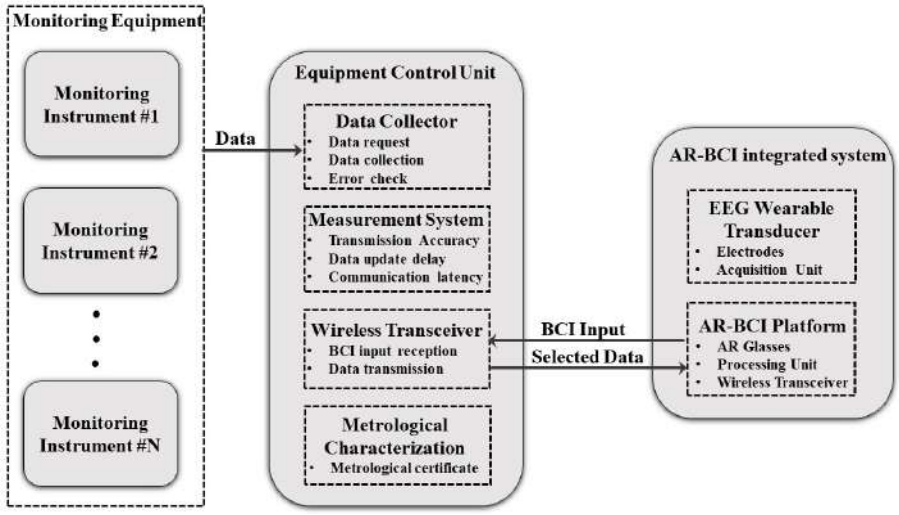

Fig. 1: Concept architecture of the proposed AR-BCI monitoring system.

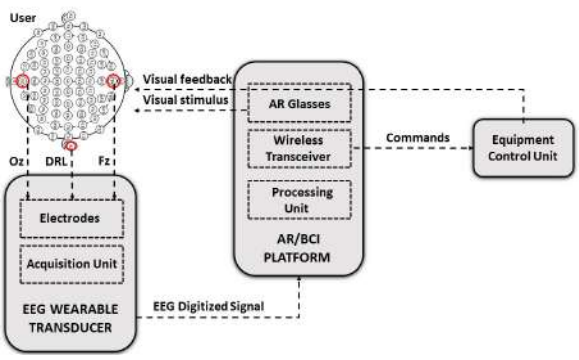

Fig. 2: AR-BCI architecture based on the SSVEP paradigm.

3.3.2. SSVEP Processing

The *EEG Digitized Signal* is sent to the processing unit to provide the information received from the *Acquisition Unit*. The result of the processing is received by the *ECU* by means of the *Wireless Transceiver*: this step allows the user to see through the *AR Glasses* the information coming from the *Monitoring Equipment*.

Fig. 3 summarizes the SSVEP acquisition and processing. A correlation-based algorithm [36] is used to detect the frequency elicited by the observed stimulus. Given a time window of length T, the corresponding signal fragment is filtered using a band-pass finite impulse response (FIR) filter between 5 Hz and 25 Hz. Then, the filtered signal fragment is correlated with four sine waveforms Φ_i where $i = 1, ..., 4$. Each waveform has a frequency corresponding to a flickering visual stimulus, and variable phase ϕ, obtaining the maximum values among the Pearson correlation coefficients ρ_i where $i = 1, ..., 4$, as expressed by the following equation:

$$\rho_i = \max_{\phi \in [0,2\pi]} \frac{cov(D_f, \Phi_i(\phi))}{\sigma_{D_f}\, \sigma_{\Phi_i(\phi)}} \quad (1)$$

where D_f are the filtered Data; Φ_i represents the ith sinewave; ϕ is the phase; σ_D is the standard deviation of the filtered data; and σ_{Φ_i} is the standard deviation of the sinewaves.
Hence, the following features are extracted:

$$F1 = 1^{st} \max_{i \in [1,4]} (\rho_i) \quad (2)$$

$$F2 = 2^{nd} \max_{i \in [1,4]} (\rho_i) \quad (3)$$

$$F3 = \frac{F1 - F2}{F2} \quad (4)$$

where $F1$ represents the maximum value among the correlation coefficients for all the four frequencies; $F2$ is the second largest correlation coefficient corresponding to one of the remaining three frequencies of stimuli; and, finally, $F3$ represents the relative difference between $F1$ and $F2$.
Given any two threshold values *T1* and *T2*, a signal fragment can be marked as recognized if the following condition is satisfied:

$$F1 > T1 \quad \cap \quad F3 > T2. \quad (5)$$

If condition (5) is not satisfied, a new fragment of duration T, overlapping with the previous one by *T/2*, is processed.

3.4. Metrological characterization of the data transmission

An off-line feature for metrological characterization, related to the communication between the devices, is included in the AR-based system. The corresponding block of *Metrological Characterization* (as shown in Fig. 1) allows to assess (i) the transmission accuracy between the ECU and the Monitoring Equipment; (ii) the data-update delay; and (iii) the communication latency.
The data-update delay depends on the communication between the *Monitoring Equipment* and the *ECU*, while the communication latency refers to the communication between the *ECU* and the *AR-BCI Integrated System*, and depends on the communication protocol used. To this aim, different experimental sessions, each consisting of several runs, are carried out automatically.

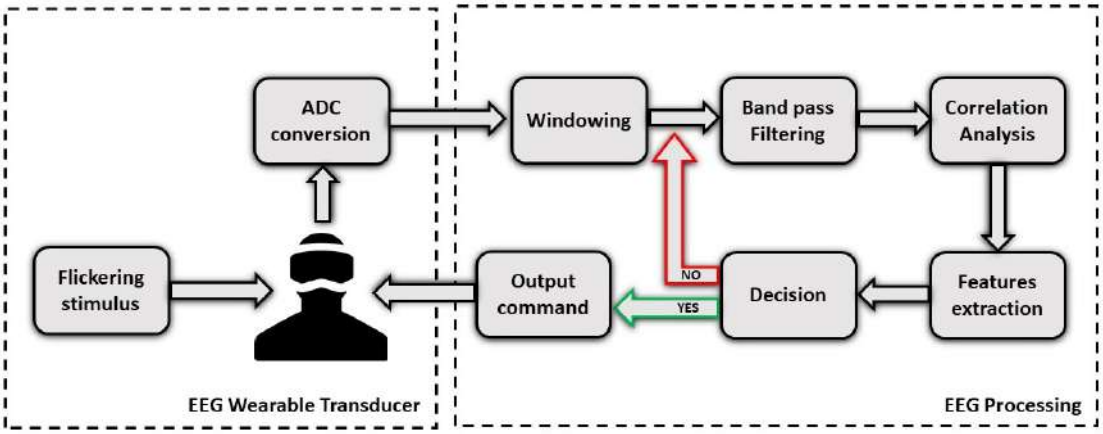

Fig. 3: Workflow of the SSVEP acquisition and processing.

For each run, the transmission accuracy, A (%), is assessed as:

$$A = \frac{N_{packets} - E}{N_{packets}} \cdot 100 \quad (6)$$

where $N_{packets}$ is the number of packets sent, and E is the error count when a packet is not correctly decoded.
Then, for each session, the accuracy mean value μ_A and the standard deviation σ_A are assessed. Hence, the 3-sigma uncertainty is computed, by taking into account the total number of runs, according to the following equation:

$$u_{\mathrm{A}} = \frac{k \cdot \sigma_{\mathrm{A}}}{\sqrt{N}} \quad (7)$$

where $k = 3$ is the coverage factor, corresponding to 99.7% confidence interval, and N is the total number of runs.

After the accuracy evaluation, the time interval necessary to update the data coming from the monitoring isntruments is measured. In particular, the time related to: (i) data-update, and (ii) wireless communication is assessed for each packet sent within a run. At the end of each run, the mean value and the standard deviation of these quantities are evaluated.
Successively, at the end of the session, the weighted mean and the 3-sigma uncertainty are assessed, considering the different number of packets sent for each run, in order to give the best estimate of the measurand. In particular, the weighted mean of the time delay μ_{t} is evaluated through the following equation:

$$\mu_{\mathrm{t}} = \frac{\sum_{i=1}^{N} \mu_{ti} \cdot l_i}{\sum_{i=1}^{N} l_i} \quad (8)$$

where μ_{ti} is the mean of the time delay evaluated for each run; and l_i is the number of packets for each run. The evaluation of the 3-sigma uncertainty is carried out taking into account the law of propagation of uncertainty.
Assuming μ_t as the weighted mean among the runs, as defined by (8), the uncertainty is evaluated through the following equation:

$$u_{\mathrm{tpr}} = \sqrt{\sum_{i=1}^{N} \left(\frac{\partial \mu_t}{\partial \mu_{ti}} \cdot u_{ti} \right)^2} \quad (9)$$

where u_{tpr} is the 3-sigma uncertainty (assessed through (7)) of the time delay evaluated with the law of propagation of uncertainty, assuming the independence between each run (an hypothesis considered acceptable based on the previous experimental campaigns); and u_{ti} is the uncertainty of the time delay evaluated for each run.
When the metrological self-characterization of the system is completed, a metrological report, summarizing the (i) transmission accuracy, (ii) the data-update delay, and (iii) the communication latency is produced for the user.

4. Implementation

As mentioned in the introduction, for the implementation, a specific healthcare-related scenario was considered. In fact, the medical environment is generally very demanding in terms of real-time requirements; hence, it represents an optimal testbed for the proposed system. The proposed AR-BCI system was implemented to be used in the operating room, to allow the OR operators (and, in particular, the anesthetist) to monitor in real-time through AR glasses the patient's vitals acquired from the OR equipment. The user interacts with a BCI to select which vital parameters he/she wants to be displayed.
This section describes the implementation of the proposed system. In particular, more details are given about
(i) the *ECU*;
(ii) the *OR Equipment*; and
(iii) the *AR-BCI Integrated System*, from the AR Glasses to the BCI Hardware.
The implementation of the system and the experimental tests were carried out at the Academic Hospital of Federico II University (Naples, Italy), employing monitoring equipment available in the operating room.

4.1. ECU

For the implementation of the system, a laptop was used as an *ECU*. The laptop has an AMD A10-9600P Processor, 16 GB RAM, and two USB 2.0 ports, which are used to communicate with the *OR Equipment* and the *AR-BCI Integrated System*. A WiFi technology *IEEE 802.11a/b/g/n* is also provided

(a) (b)

Fig. 4: OR Equipment: a) Drager Evita Infinity V500 ventilator; b) Philips IntelliVue MP90 patient monitor.

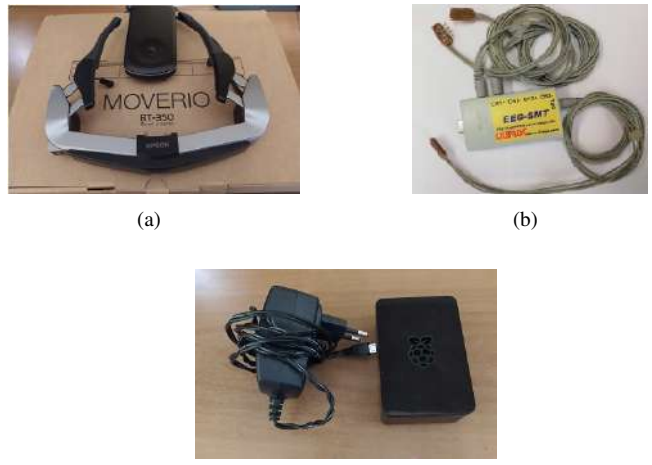

(a) (b)

(c)

Fig. 5: AR-BCI Equipment: a) Moverio BT-350; b) Olimex EEG-SMT; c) Raspberry Pi 3.

for the wireless communication with the aforementioned system blocks. A software running in MATLAB environment collects the data from the *OR Equipment*, checks if any error has occurred, and sends the data to the *AR-BCI Integrated System*, according to the user's selection. Moreover, the developed software provides a measurement of the transmission performance in terms of accuracy, data update and communication delay.

4.2. OR equipment

For the implementation of the proposed system, two electromedical instruments were used, namely a ventilator for intensive care and a patient monitor: these are pieces of equipment that are typically available in the OR [37].

- *Ventilator*: Fig. 4(a) shows a picture of the mechanical ventilator used for the implementation, namely the Drager Evita Infinity V500 [66]. This ventilator is equipped with a LAN interface and three serial interfaces, and it is possible to fetch the parameters using the MEDIBUS protocol at different Baud Rates.

- *Monitor*: Fig. 4(b) shows the monitor used for the implementation, namely the Philips IntelliVue MP90 [67]. IntelliVue MP90 has a conventional diagnostic 12-lead ECG, arrhythmia, arterial blood pressure and oxygen saturation analysis. It is equipped with a LAN interface; data are collected by means of a dedicated proprietary software, namely *Medicollector*.

In this application, the vital signs coming from the instrumentation are collected by the laptop, which communicates (i) with the Ventilator over MEDIBUS protocol via RS-232 to USB adapter, and (ii) with the Monitor via Medicollector adapter, a LAN to RS-232 adapter. To establish a LAN-USB connection between the patient monitor and the laptop, an additional RS-232 to USB adapter was used. The parameters acquired from the instruements are displayed in real-time on the AR glasses which receive wirelessly the data collected from the laptop.

4.3. AR-BCI integrated system

The AR-BCI integrated system was implemented using components off-the-shelf. It includes
(i) a pair of *AR Glasses*;
(ii) *Electrodes* and *Acquisition Unit*, constituting the *EEG Wearable Transducer* in Fig. 2; and
(iii) a *Processing Unit*, integrating the *Wireless transceiver*.

- *AR glasses*: In this work, the Epson Moverio BT-350 [68] glasses were used (Fig. 5(a)). This is an AR optical see-through (OST) device with a 30 Hz nominal refresh rate; an angle of view of 23 degrees diagonally; and a *720p* display. These AR smart glasses are equipped with Android 5.1. A dedicated Android application was developed and built with a twofold aim: (i) for generating the flickering visual stimuli for the BCI-based input; and (ii) for receiving and displaying in real-time the vital signs from the OR equipment

- *Electrodes and Acquisition Unit:* the Olimex EEG-SMT was used as an Acquisition Unit [69], a 10-bit, 256 Sa/s, differential input Analog-Digital Converter (ADC). The electrodes and the Olimex are shown in Fig. 5(b).

- *Processing Unit:* This includes a Raspberry Pi 3 (Fig. 5(c) [70]), connected via USB to the Acquisition Unit. The Raspberry Pi 3 is also used as a *Wireless Transceiver*, to communicate the results of the SSVEP detection to the laptop. In this way, the user is capable to move smoothly in the OR thanks to the high wearability.

Overall, this configuration of the AR-BCI System represents a single-channel BCI, which guarantees:
(i) high wearability, thanks to the low number of EEG electrodes and the small dimensions of the hardware used, and
(ii) high accuracy and low latency, even employing low-cost hardware.

4.4. Communication

Dedicated software was developed to handle (i) the communication between the laptop and the OR Equipment; (ii) the communication between the EEG Acquisition Unit and the EEG Processing Unit; (iii) the communication between the EEG Processing Unit and the laptop; and (iv) the communication between the laptop and the AR Smart Glasses. Fig. 6 describes in detail the communication between the devices.

(i) Communication between the laptop and the Equipment: A code running in MATLAB environment was developed to implement the acquisition from the instrumentation and sending of the data. A subsection of the MATLAB code implemented the MEDIBUS protocol at a Baud rate of 38400 bit/s to configure and receive in real-time the ventilator parameters. Furthermore, a second subsection is in charge of exchanging data with Medicollector (i.e., the proprietary softwaref for acquiring the waveform from the monitor). While Medicollector is running on the laptop, the MATLAB code acquire in real-time the desired Monitor waveforms over TCP/IP protocol.

(ii) Communication between the EEG Acquisition Unit and the EEG Processing Unit: The digitized EEG signal is sent via USB to the EEG Processing Unit. The software installed on the Processing Unit is written in C, and acquires via UART the EEG signal digitized by the Acquisition Unit. The Baud Rate is set to 57600 bit/s, the packet size is equal to 17 bytes, and no parity bit is foreseen. The software also provides the function of TCP Client, sending to the laptop (acting as a TCP Server) the result of the processing.

(iii) Communication between the EEG Processing Unit and the laptop: For the laptop, a TCP Server was implemented and integrated in MATLAB with the code for the acquisition of the parameters from the OR equipment. The TCP Server is used to establish the communication with the EEG Processing Unit. Once the connection with the the Processing Unit (acting as a TCP Client) is initialized, the Server receives the results of the processing over TCP/IP protocol. Consequently, the laptop sends to the Glasses the parameters according to the user's selection.

(iv) Communication between the laptop and the Glasses: The aforementioned TCP Server is also used to establish the communication between the laptop and the Glasses. Once the connection with the the AR Glasses (acting as a TCP Client) is established, the laptop (Server) can send the parameters to the user over TCP/IP protocol. An Android application developed in Android Studio is implemented to receive over TCP/IP protocol the vital signs, and display them in real-time.

5. Preliminary metrological characterization of BCI-SSVEP

Before proceeding with the experimental validation and metrological characterization of the proposed system, an offline analysis of the BCI dataset was carried out. With respect to [36], this analysis was focused on taking into account the effect of frame rate drop in the visualization of the flickering stimuli.

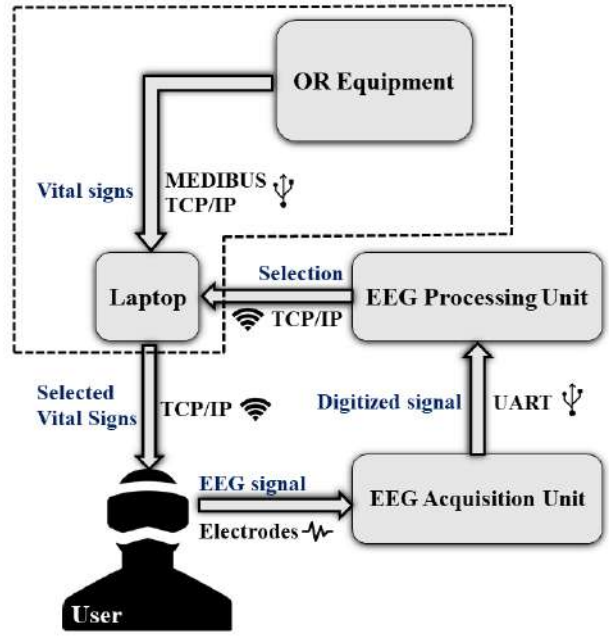

Fig. 6: Details of the communication between the devices.

The analysis of the performance of the BCI-SSVEP system allowed to assess the accuracy and the latency of the SSVEP detection algorithm, compared with the demanded requirements for medical application.

The accuracy A is defined as the number of signal fragments correctly classified, divided by the total number of signals, and it is typically expressed as a percentage, as in (6).
On the other hand, the latency is the time needed by the algorithm to classify a signal fragment.

Brain signals of 20 healthy and untrained volunteers were analyzed, after acquiring 24 brain signals per subject.
It should be mentioned that for creating the dataset, the Epson Moverio BT-200 was used as *AR Glasses*, with a nominal refresh rate of 60 Hz. While the AR glasses used for the experiments at the Federico II Hospital were the Epson Moverio BT-350. Nevertheless, thanks to the modularity of the system, this does not represent an issue because the only parameter that changes for the SSVEP stimuli generation and detection is the refresh rate, which has a nominal value of 60 Hz for the Moverio BT-200 and a nominal value of 30 Hz for the Moverio BT-350. However, for practical applications, the Moverio BT-350 represents a better choice because it is more powerful in terms of CPU and RAM: this translates into a better stability of the frame rate.

The luminosity of the environment was (97 ± 2) lx. In this characterization, two stimuli were used, at a nominal frequency of 10.0 Hz and 12.0 Hz. Each subject was asked to focus on one stimulus at a time, for 10 s. After collecting the acquired data, an analysis of the frame rate drop was carried out, obtaining an average frame rate of approximately 59.0 Hz. This leads to a shift of the stimuli frequency from 12.0 Hz to 11.8 Hz. By taking into account this shift, the new performances were evaluated. In Table 1 and Tab. 2 the accuracy and the latency values measured at 3-σ (99.7% confidence level) as a function of T

Table 1: 3-σ Accuracy (%) of SSVEP detection algorithm for different time windows T and threshold values T1.

		T1					
		0.50	**0.52**	**0.54**	**0.56**	**0.58**	**0.60**
T (s)	**0.5**	79.6 ± 9.7	81.0 ± 9.3	82.7 ± 8.3	83.3 ± 8.3	83.7 ± 8.0	85.7 ± 7.8
	0.6	86.0 ± 7.9	86.4 ± 8.2	87.2 ± 8.1	87.7 ± 8.1	88.6 ± 7.6	89.7 ± 6.8
	0.8	91.0 ± 6.2	90.7 ± 6.5	91.2 ± 6.6	93.3 ± 4.7	93.9 ± 4.4	94.6 ± 4.6
	1.0	93.8 ± 6.0	95.0 ± 5.4	94.2 ± 5.9	96.1 ± 3.4	96.0 ± 3.7	96.9 ± 3.8

Table 2: 3-σ Time response (s) of SSVEP detection algorithm for different time windows T and threshold values T1.

		T1					
		0.50	**0.52**	**0.54**	**0.56**	**0.58**	**0.60**
T (s)	**0.5**	1.23 ± 0.13	1.30 ± 0.13	1.45 ± 0.16	1.58 ± 0.18	1.82 ± 0.22	2.16 ± 0.25
	0.6	1.61 ± 0.18	1.81 ± 0.21	1.99 ± 0.23	2.28 ± 0.27	2.55 ± 0.29	2.85 ± 0.32
	0.8	2.54 ± 0.27	2.85 ± 0.30	3.16 ± 0.32	3.50 ± 0.35	4.01 ± 0.37	4.46 ± 0.37
	1.0	3.42 ± 0.31	3.82 ± 0.33	4.17 ± 0.34	4.73 ± 0.37	5.13 ± 0.38	5.72 ± 0.38

Table 3: SSVEP detection algorithm for T = 0.8 s and $T1$ = 0.56.

Volunteer	Accuracy (%)	Latency (s)
#1	91.7	2.85 ± 1.39
#2	95.5	3.71 ± 1.97
#3	73.7	4.55 ± 2.08
#4	100.0	1.96 ± 0.68
#5	95.5	3.30 ± 1.65
#6	95.5	4.73 ± 1.68
#7	100.0	1.55 ± 0.60
#8	94.4	5.23 ± 1.95
#9	95.8	1.40 ± 0.80
#10	95.8	1.95 ± 0.73
#11	95.8	1.00 ± 0.26
#12	91.7	1.78 ± 0.69
#13	100.0	6.05 ± 1.82
#14	95.2	4.28 ± 2.00
#15	95.8	1.53 ± 0.64
#16	100.0	6.10 ± 2.39
#17	87.0	3.06 ± 1.15
#18	76.5	5.50 ± 2.07
#19	95.5	4.93 ± 1.83
#20	90.9	4.56 ± 1.81
Results	93.3 ± 4.7	3.50 ± 0.35

and $T1$ are evaluated. The threshold $T2$ was set to 0.5, which means that the feature $F1$ must be at least the 50% greater than the feature $F2$.
A focus on the SSVEP detection algorithm for T = 0.8 s and $T1$ = 0.56 is given in Table 3. These two threshold values were chosen so as to guarantee an accuracy compatible with the healthcare requirements. In particular, the SSVEP recognition reaches an accuracy of about 93.3 % with a Latency of about 3.50 s.

For comparison, Fig. 7 shows the the difference in terms of accuracy and latency between the current analysis and the one reported in [36]. It can be noticed that, between 2 s and 4 s the accuracy rises by approximately 1.5 %.

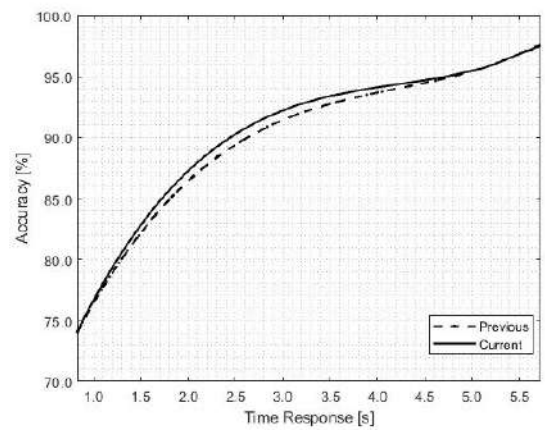

Fig. 7: Accuracy of SSVEP processing: comparison of the results from this preliminary analysis and the results reported in [36].

6. Experimental results

First, the system functionality was validated, with a focus on the frame rate drop related to the generation of the flickering stimuli. Then, the on field results related to the BCI accuracy and latency were obtained. Furthermore, the performances of the BCI System with four flickering stimuli are discussed. Successively, the reliability of the proposed AR-BCI integrated monitoring system was evaluated by measuring the accuracy of the transmission, and the delay time needed by the display to be updated with the vital parameters acquired from the OR equipment.

6.1. Functional Validation

The preliminary validation was carried out to ensure each block of the system architecture worked properly.
In the experiments, the patient's lung was emulated by means of a non-self-inflating bag plugged to the Ventilator. The MEDIBUS communication was established with a Baud Rate set to 38500 bit/s. The patient monitor was used to monitor the vitals of a healthy volunteer. Table 4 summarizes the set of parameters that were collected.

Table 4: Vitals monitored during the experimental tests.

Parameter	Symbol	Unit	Ventilator/Monitor
Compliance	Cdyn	l/bar	Ventilator
Minimum Airway Pressure	Pmin	mbar	Ventilator
Mean Airway Pressure	Pmean	mbar	Ventilator
Peak Airway Pressure	PIP	mbar	Ventilator
Minute Volume	MV	l/min	Ventilator
Spontaneous expired total volume	VTespon	ml	Ventilator
O_2 Saturation	SpO2	%	Monitor
Compound ECG	ECG	mV	Monitor
Respiratory Rate	RR	1/min	Monitor
Hearth Rate	FC	1/min	Monitor

Fig. 8: Picture of the user wearing the AR-BCI system.

Fig. 9: Flickering squares to select waveforms.

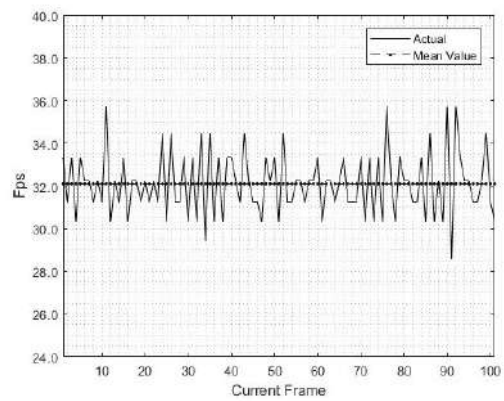

Fig. 10: Moverio BT-350 frame rate while running the Android application.

6.2. Operation

Fig. 8 shows a picture of the user wearing the AR Glasses and electrodes, with the OR Equipment in background.
Once the laptop and the OR equipment are connected via cable, the MATLAB code and the Medicollector software can be launched. The user launches the dedicated Android application and inserts the Server IP address and Port number. Then, four squares flickering at different frequencies appear on the AR glasses display, as shown in Fig. 9. Each square corresponds to the selection of a waveform coming from the patient monitor; in the considered case, the possible selection was among Electrocardiogram (ECG), Oxygen Saturation (O2Sat), Respiration Rate (RR), and Heart Rate (HR).

Before acquiring the SSVEP elicited by the flickering stimuli generated by the Moverio BT-350, the effort needed by the system to produce each time a new frame was measured, obtaining an average frame rate of about 32 fps, higher than the 30 Hz of BT-350 nominal refresh rate. This leads to the presence of undesired multiple frames. Therefore, the code working on the Android application and related to the rendering of the visual stimuli was modified taking into account the average fps obtained. Fig. 10 shows the variation of the fps while the Android application is in execution.

After executing the code on the Raspberry, the acquisition and processing of the EEG signal starts. The Raspberry sends the results of the processing to the laptop and, finally, the laptop forwards the collected parameters (as selected by the user) to the AR glasses. Fig. 11 shows a snapshot of what the user sees after selecting the ECG waveform by SSVEP. The user sees the main parameters from the ventilator and, at the bottom, the real-time variation of ECG. In this way, the user has complete control of the information.

6.3. Experimental characterization of the BCI performance

After validating the functionalities of the system in relation to (i) the acquisition and visualization of the vital signs and (ii) to the rendering of the flickering stimuli and the EEG processing, the on-field BCI performance was assessed. The flickering frequencies chosen to let the user select the waveforms coming from the patient monitor were 8 Hz, 10 Hz, 12 Hz and 15 Hz.
At each run, the user was asked to declare which visual stimulus he was looking at. Table 6 summarizes the user's answers, with the time needed by the algorithm to detect the SSVEP. It was observed that, in three cases, the algorithm could not identify the correct frequency observed.
As reported in Table 6, the frequency value that showed the best performance in terms of both accuracy and latency was 8 Hz; this is due to the fact that the highest frequency values are more sensitive to the frame rate drop. For instance, a frame rate drop from 32.0 Hz to 30.0 Hz leads to a frequency shift from 15.0 Hz to 14.1 Hz, and from 8.0 Hz to 7.5 Hz. Therefore, the SSVEP detection has a higher probability of success at 8 Hz and 10 Hz, rather than at 12 and 15 Hz. Moreover, the luminosity of the environment (147 ± 2) lx and the presence of four squares instead of two, also contributed to the drop of the overall accuracy with respect to the results obtained in Section 5. After the user made

Fig. 11: Snapshot of the user's view after the BCI-made selection.

the selection through BCI, the vital signs are displayed on the AR Smart Glasses.

6.4. Metrological characterization of the system transmission

The experimental session consisted in 10 runs. As the Medicollector was in free-trial mode, each run had a maximum duration of 180 s. For each run, the measurement of the transmission accuracy was carried out through (6). Then, the mean value and the 3-sigma uncertainty were evaluated taking into account the total number of runs.

Finally, the system's delay time, namely the time interval necessary to update the data coming from the devices, was measured by means of the MATLAB stopwatch timer *tic*.

For each packet within a run, it was possible to evaluate the delay related to: (i) ventilator update, (ii) monitor update, and (iii) TCP communication. Based on previous experimental campaigns carried out by the authors [37], the TCP/IP delay was considered negligible; in fact, its value is typically lower than than 2 ms, which fully satisfies the requirements expressed in [41, 42]). For this reason, only the mean value and the standard deviation related to the Monitor and Ventilator update delay were reported at the end of each run. At the end of the session, the assessment of the weighted mean and of the 3-σ propagated uncertainty was carried out (This was done taking into account the different number of packets sent for each run). In particular, the weighted mean of the data-update delay (μ_t) was evaluated through (8). The standard deviation and, consequently, the 3-sigma uncertainty, were evaluated according to the law of propagation of uncertainty, assuming the independence of each run, as shown in (9).

Table 5: Results of BCI processing in terms of accuracy and latency for each run during the experimental session.

#Run	Frequency [Hz]	[0-2 s]	[2-4 s]	[4-6 s]
#1	8 Hz	✓		
#2	10 Hz		✓	
#3	12 Hz		✓	
#4	15 Hz			✓
#5	8 Hz	✓		
#6	10 Hz	✓		
#7	12 Hz			✗
#8	15 Hz		✗	
#9	8 Hz		✓	
#10	10 Hz			✗

Table 6: Summary of BCI performance after the experimental session.

Frequency [Hz]	Accuracy [%]	Mean latency [s]
8 Hz	100.0	2.67
10 Hz	66.7	4.00
12 Hz	50.0	5.00
15 Hz	50.0	5.00
Total	**70.0**	**4.00**

Table 7 summarizes the details of the experimental session, considering the delay related to the Monitor and Ventilator parameters update, along with the Accuracy of the transmission. It can be noticed that the accuracy related to the TCP/IP transmission is 100.0%: no errors occurred during the whole test.

Table 7: Details for each run of the experimental session.

#Packets	Mean Delay [s]	Std Delay [s]	Accuracy [%]
(i) 149	0.97	0.19	98.0
(ii) 75	1.95	0.37	100.0
(i) 150	1.01	0.22	96.7
(ii) 78	1.98	0.39	100.0
(i) 145	0.95	0.17	97.2
(ii) 75	1.87	0.44	100.0
(i) 156	0.98	0.19	96.1
(ii) 80	1.95	0.39	100.0
(i) 139	0.99	0.21	97.8
(ii) 73	1.92	0.40	100.0
(i) 143	0.97	0.19	98.0
(ii) 73	1.92	0.45	100.0
(i) 132	0.97	0.19	96.2
(ii) 69	1.89	0.47	100.0
(i) 131	0.99	0.21	99.2
(ii) 68	1.93	0.44	100.0
(i) 122	0.96	0.19	97.5
(ii) 62	1.94	0.39	100.0
(i) 126	0.99	0.21	97.6
(ii) 66	1.93	0.43	100.0
TOTAL	**Weighted Mean [s]**	**Propagated Unc [s]**	**Mean ± Unc [%]**
(i) 1393	0.98	0.02	97.4 ± 0.9
(ii) 719	1.92	0.05	100.0 ± 0.0

Legend:
(i) Drager update
(ii) Philips update

7. Conclusion

An integrated BCI-AR real-time monitoring system for the acquisition and visualization of data from *Monitoring equipment* was proposed. The system, which relies on the combination of BCI and AR to allow the user to select hands-free which data they want to display in AR, was implemented and validated considering a healthcare application scenario.

In particular, as a case study, the real-time AR-based visualization of patient's vitals was considered. The data are acquired from the OR equipment in real-time, and displayed on the user's AR glasses. The user can select hands-free which parameter should be displayed on the AR glasses, by means of a highly-wearable, noninvasive and trainingless SSVEP-based BCI.

The overall system was designed, implemented and validated

through experimental tests using the equipment typically available in the OR. After a preliminary functional validation, the system accuracy and delay were assessed for both the BCI and the AR subsystems, thus demonstrating the effectiveness and reliability of the proposed AR-BCI-based monitoring system. The obtained measured transmission accuracy of the vital signs is higher than 97%, with a negligible delay introduced by the Android application to receive the parameters, preserving the reliability and real-time requirements that the contexts necessitates and confirming the improvement of AR in the Health 4.0 framework. The on-the-field performance of the single-channel SSVEP-based BCI showed an accuracy of 70% with a latency of approximately 4.00 s. Further work will be dedicated to improve the SSVEP-detection algorithm: in particular, the introduction of a time-frequency analysis in the processing could mitigate the effects caused by the frame-rate drop, thus improving the overall results.

Acknowledgment

This work was carried out as part of the ”ICT for Health” project, which was financially supported by the Italian Ministry of Education, University and Research (MIUR), under the initiative ‘Departments of Excellence’ (Italian Budget Law no. 232/2016), through an excellence grant awarded to the Department of Information Technology and Electrical Engineering of the University of Naples Federico II, Naples, Italy.

The authors would like to thank prof. Lucio De Paolis (University of Salento) for his advice on the design of the AR application; Ernesto Erra (Univesity of Naples Federico II) for the support in implementing the application; and Dr. Maria Vargas (University of Naples Federico II) for her support in the experimental validation at the University Hospital.

References

[1] Wehde, M.. Healthcare 4.0. IEEE Engineering Management Review 2019;47(3):24–28. doi:10.1109/EMR.2019.2930702.

[2] Forum, W.E.. Health and healthcare in the fourth industrial revolution global future council on the future of health and healthcare 2016-2018. 2019. URL: http://www3.weforum.org/docs/WEF_Shaping_the_Future_of_Health_Council_Report.pdf.

[3] Zhang, Y., Cui, J., Ma, K., Chen, H., Zhang, J.. A wristband device for detecting human pulse and motion based on the internet of things. Measurement 2020;163:108036. doi:10.1016/j.measurement.2020.108036.

[4] Angrisani, L., Arpaia, P., Moccaldi, N., Esposito, A.. Wearable augmented reality and brain computer interface to improve human-robot interactions in smart industry: A feasibility study for ssvep signals. In: IEEE 4th International Forum on Research and Technologies for Society and Industry, RTSI 2018 - Proceedings. 2018, p. 1–5. doi:10.1109/RTSI.2018.8548517.

[5] Angrisani, L., Arpaia, P., Esposito, A., Moccaldi, N.. A wearable brain-computer interface instrument for augmented reality-based inspection in industry 4.0. IEEE Transactions on Instrumentation and Measurement 2019;69(4). doi:10.1109/TIM.2019.2914712.

[6] Amoon, M., Altameem, T., Altameem, A.. Internet of things sensor assisted security and quality analysis for health care data sets using artificial intelligent based heuristic health management system. Measurement 2020;161:107861. doi:10.1016/j.measurement.2020.107861.

[7] Fouad, H., Hassanein, A.S., Soliman, A.M., Al-Feel, H.. Analyzing patient health information based on iot sensor with ai for improving patient assistance in the future direction. Measurement 2020;159:107757. doi:10.1016/j.measurement.2020.107757.

[8] Uçar, M.K., Uçar, Z., Köksal, F., Daldal, N.. Estimation of body fat percentage using hybrid machine learning algorithms. Measurement 2021;167:1–13.

[9] Abdelaziz, A., Elhoseny, M., Salama, A.S., Riad, A.. A machine learning model for improving healthcare services on cloud computing environment. Measurement 2018;119:117 – 128. doi:10.1016/j.measurement.2018.01.022.

[10] Zadpoor, A., Malda, J.. Additive manufacturing of biomaterials, tissues, and organs. Annals of Biomedical Engineering 2017;45(1). doi:10.1007/s10439-016-1719-y.

[11] Cosoli, G., Spinsante, S., Scalise, L.. Wrist-worn and chest-strap wearable devices: Systematic review on accuracy and metrological characteristics. Measurement 2020;159:107789. doi:10.1016/j.measurement.2020.107789.

[12] Corchia, L., Monti, G., Tarricone, L.. Wearable antennas: Nontextile versus fully textile solutions. IEEE Antennas and Propagation Magazine 2019;61(2):71–83. doi:10.1109/MAP.2019.2895665.

[13] Corchia, L., Monti, G., Raheli, F., Candelieri, G., Tarricone, L.. Dry textile electrodes for wearable bio-impedance analyzers. IEEE Sensors Journal 2020;20(11):6139–6147. doi:10.1109/JSEN.2020.2972603.

[14] Schiavoni, R., Monti, G., Piuzzi, E., Tarricone, L., Tedesco, A., De Benedetto, E., et al. Feasibility of a wearable reflectometric system for sensing skin hydration. Sensors 2020;20(10). doi:10.3390/s20102833.

[15] Gattullo, M., Scurati, G.W., Fiorentino, M., Uva, A.E., Ferrise, F., Bordegoni, M.. Towards augmented reality manuals for industry 4.0: A methodology. Robotics and Computer-Integrated Manufacturing 2019;56:276–286.

[16] Ullo, S.L., Piedimonte, P., Leccese, F., De Francesco, E.. A step toward the standardization of maintenance and training services in c4i military systems with mixed reality application. Measurement 2019;138:149–156.

[17] Haque, S.A., Aziz, S.M., Rahman, M.. Review of cyber-physical system in healthcare. international journal of distributed sensor networks 2014;10(4):217415.

[18] Jimenez, J., Jahankhani, H., Kendzierskyj, S.. Health care in the cyberspace: Medical cyber-physical system and digital twin challenges. Internet of Things 2020;:79–92doi:10.1007/978-3-030-18732-3_6.

[19] Tedesco, A., Gallo, M., Tufano, A.. A preliminary discussion of measurement and networking issues in cyber physical systems for industrial manufacturing. In: 2017 IEEE International Workshop on Measurement and Networking (M&N) Proceedings. 2017,doi:10.1109/IWMN.2017.8078384.

[20] Wolpaw, J.R., Birbaumer, N., McFarland, D.J., Pfurtscheller, G., Vaughan, T.M.. Brain–computer interfaces for communication and control. Clinical neurophysiology 2002;113(6):767–791.

[21] Wolpaw, J.R., Birbaumer, N., Heetderks, W.J., McFarland, D.J., Peckham, P.H., Schalk, G., et al. Brain-computer interface technology: a review of the first international meeting. IEEE transactions on rehabilitation engineering 2000;8(2):164–173.

[22] Hu, K., Chen, C., Meng, Q., Williams, Z., Xu, W.. Scientific profile of brain–computer interfaces: Bibliometric analysis in a 10-year period. Neuroscience letters 2016;635:61–66.

[23] Kerous, B., Skola, F., Liarokapis, F.. Eeg-based bci and video games: a progress report. Virtual Reality 2018;22(2):119–135.

[24] Perrin, X., Chavarriaga, R., Colas, F., Siegwart, R., Millán, J.d.R.. Brain-coupled interaction for semi-autonomous navigation of an assistive robot. Robotics and Autonomous Systems 2010;58(12):1246–1255.

[25] Sanchez-Fraire, U., Parra-Vega, V., Martinez-Peon, D., Sepúlveda-Cervantes, G., Sanchez-Orta, A., Muñoz-Vázquez, A.. On the brain computer robot interface (bcri) to control robots. IFAC-PapersOnLine 2015;48(19):154–159.

[26] Abdulkader, S.N., Atia, A., Mostafa, M.S.M.. Brain computer interfacing: Applications and challenges. Egyptian Informatics Journal 2015;16(2):213–230.

[27] Kersten-Oertel, M., Jannin, P., Collins, D.. Dvv: A taxonomy for mixed reality visualization in image guided surgery. IEEE Transactions on Visualization and Computer Graphics 2012;18(2):332–352. doi:10.1109/TVCG.2011.50.

[28] De Paolis, L.T.. Augmented visualization as surgical support in the treatment of tumors. In: International Conference on Bioinformatics and Biomedical Engineering. Springer; 2017, p. 432–443.

[29] De Paolis, L.T., De Luca, V.. Augmented visualization with depth perception cues to improve the surgeon's performance in minimally invasive

surgery. Medical & biological engineering & computing 2019;57(5):995–1013.

[30] Bernhardt, S., Nicolau, S.A., Soler, L., Doignon, C.. The status of augmented reality in laparoscopic surgery as of 2016. Medical image analysis 2017;37:66–90.

[31] Mamone, V., Condino, S., Cutolo, F., Tamadon, I., Menciassi, A., Murzi, M., et al. Low-computational cost stitching method in a three-eyed endoscope. Journal of Healthcare Engineering 2019;2019.

[32] Ormerod, D., Ross, B., Naluai-Cecchini, A.. Use of an augmented reality display of patient monitoring data to enhance anesthesiologists' response to abnormal clinical events. Studies in Health Technology and Informatics 2003;94:248–250. doi:10.3233/978-1-60750-938-7-248.

[33] Sanderson, P.M., Watson, M.O., Russell, W.J., Jenkins, S., Liu, D., Green, N., et al. Advanced auditory displays and head-mounted displays: advantages and disadvantages for monitoring by the distracted anesthesiologist. Anesthesia & Analgesia 2008;106(6):1787–1797.

[34] McDuff, D., Hurter, C., Gonzalez-Franco, M.. Pulse and vital sign measurement in mixed reality using a hololens. In: Proceedings of the 23rd ACM Symposium on Virtual Reality Software and Technology. 2017, p. 1–9.

[35] Putze, F., Vourvopoulos, A., Lécuyer, A., Krusienski, D., Bermúdez i Badia, S., Mullen, T., et al. Editorial: Brain-computer interfaces and augmented/virtual reality. Frontiers in Human Neuroscience 2020;14. doi:10.3389/fnhum.2020.00144.

[36] Arpaia, P., Duraccio, L., Moccaldi, N., Rossi, S.. Wearable brain-computer interface instrumentation for robot-based rehabilitation by augmented reality. IEEE Transactions on Instrumentation and Measurement 2020;69(9):6362–6371. doi:10.1109/TIM.2020.2970846.

[37] Arpaia, P., De Benedetto, E., Dodaro, C.A., Duraccio, L., Servillo, G.. Metrology-based design of a wearable augmented reality system for monitoring patient's vitals in real time. IEEE Sensors Journal 2021;doi:10.1109/JSEN.2021.3059636; to be publised.

[38] Arpaia, P., Moccaldi, N., Prevete, R., Sannino, I., Tedesco, A.. A wearable eeg instrument for real-time frontal asymmetry monitoring in worker stress analysis. IEEE Transactions on Instrumentation and Measurement 2020;69(10). doi:10.1109/TIM.2020.2988744.

[39] Mihajlović, V., Grundlehner, B., Vullers, R., Penders, J.. Wearable, wireless eeg solutions in daily life applications: what are we missing? IEEE journal of biomedical and health informatics 2014;19(1):6–21.

[40] Braud, T., Bijarbooneh, F.H., Chatzopoulos, D., Hui, P.. Future networking challenges: The case of mobile augmented reality. In: 2017 IEEE 37th International Conference on Distributed Computing Systems (ICDCS). IEEE; 2017, p. 1796–1807.

[41] Sze, H., Liew, S.C., Lee, J.Y., Yip, D.C.. A multiplexing scheme for h. 323 voice-over-ip applications. IEEE Journal on Selected Areas in Communications 2002;20(7):1360–1368.

[42] Feng, S., Liang, Z., Zhao, D.. Providing telemedicine services in an infrastructure-based cognitive radio network. IEEE Wireless Communications 2010;17(1):96–103.

[43] Alesanco, A., García, J.. Clinical assessment of wireless ecg transmission in real-time cardiac telemonitoring. IEEE Transactions on Information Technology in Biomedicine 2010;14(5):1144–1152.

[44] Muhammed, T., Mehmood, R., Albeshri, A., Katib, I.. Ubehealth: a personalized ubiquitous cloud and edge-enabled networked healthcare system for smart cities. IEEE Access 2018;6:32258–32285.

[45] Angrisani, L., Arpaia, P., Casinelli, D., Moccaldi, N.. A single-channel ssvep-based instrument with off-the-shelf components for training brain-computer interfaces. IEEE Transactions on Instrumentation and Measurement 2018;68(10):3616–3625.

[46] Ramadan, R.A., Vasilakos, A.V.. Brain computer interface: control signals review. Neurocomputing 2017;223:26–44.

[47] Donchin, E., Ritter, W., McCallum, W.C., et al. Cognitive psychophysiology: The endogenous components of the erp. Event-related brain potentials in man 1978;349:411.

[48] Dal Seno, B., Matteucci, M., Mainardi, L.. Online detection of p300 and error potentials in a bci speller. Computational intelligence and neuroscience 2010;2010.

[49] McFarland, D.J., Krusienski, D.J., Wolpaw, J.R.. Brain–computer interface signal processing at the wadsworth center: mu and sensorimotor beta rhythms. Progress in brain research 2006;159:411–419.

[50] Carretié, L.. Exogenous (automatic) attention to emotional stimuli: a review. Cognitive, Affective, & Behavioral Neuroscience 2014;14(4):1228–1258.

[51] Wang, Y., Wang, R., Gao, X., Hong, B., Gao, S.. A practical vep-based brain-computer interface. IEEE Transactions on neural systems and rehabilitation engineering 2006;14(2):234–240.

[52] Ajami, S., Mahnam, A., Abootalebi, V.. Development of a practical high frequency brain–computer interface based on steady-state visual evoked potentials using a single channel of eeg. Biocybernetics and Biomedical Engineering 2018;38(1):106–114.

[53] Wang, Y.T., Wang, Y., Jung, T.P.. A cell-phone-based brain–computer interface for communication in daily life. Journal of neural engineering 2011;8(2):025018.

[54] Cheng, M., Gao, X., Gao, S., Xu, D.. Design and implementation of a brain-computer interface with high transfer rates. IEEE transactions on biomedical engineering 2002;49(10):1181–1186.

[55] Volosyak, I., Gembler, F., Stawicki, P.. Age-related differences in ssvep-based bci performance. Neurocomputing 2017;250:57–64.

[56] Cecotti, H.. A self-paced and calibration-less ssvep-based brain–computer interface speller. IEEE Transactions on Neural Systems and Rehabilitation Engineering 2010;18(2):127–133.

[57] Sokol, S.. Visually evoked potentials: theory, techniques and clinical applications. Survey of ophthalmology 1976;21(1):18–44.

[58] Anindya, S.F., Rachmat, H.H., Sutjiredjeki, E.. A prototype of ssvep-based bci for home appliances control. In: 2016 1st International Conference on Biomedical Engineering (IBIOMED). IEEE; 2016, p. 1–6.

[59] Yin, E., Zhou, Z., Jiang, J., Yu, Y., Hu, D.. A dynamically optimized ssvep brain–computer interface (bci) speller. IEEE Transactions on Biomedical Engineering 2014;62(6):1447–1456.

[60] Martišius, I., Damaševičius, R.. A prototype ssvep based real time bci gaming system. Computational intelligence and neuroscience 2016;2016.

[61] Astaras, A., Moustakas, N., Athanasiou, A., Gogoussis, A.. Towards brain-computer interface control of a 6-degree-of-freedom robotic arm using dry eeg electrodes. Advances in Human-Computer Interaction 2013;2013.

[62] Muller-Putz, G.R., Pfurtscheller, G.. Control of an electrical prosthesis with an ssvep-based bci. IEEE Transactions on biomedical engineering 2007;55(1):361–364.

[63] Chen, X., Zhao, B., Wang, Y., Xu, S., Gao, X.. Control of a 7-dof robotic arm system with an ssvep-based bci. International journal of neural systems 2018;28(08):1850018.

[64] Wu, C.H., Lakany, H.. The effect of the viewing distance of stimulus on ssvep response for use in brain-computer interfaces. In: 2013 IEEE International Conference on Systems, Man, and Cybernetics. IEEE; 2013, p. 1840–1845.

[65] Duszyk, A., Bierzyńska, M., Radzikowska, Z., Milanowski, P., Kuś, R., Suffczyński, P., et al. Towards an optimization of stimulus parameters for brain-computer interfaces based on steady state visual evoked potentials. Plos one 2014;9(11):e112099.

[66] Ventilator Drager Infinity V500. 2020. URL: https://cardomedical.com/product/drager-evita-infinity-v500-ventilator/.

[67] Philips IntelliVue MP-90. 2020. URL: https://avantehs.com/p/philips-intellivue-mp90-patient-monitor/1511.

[68] Epson moverio bt-350 website. 2020. URL: https://www.epson.eu/products/see-through-mobile-viewer/moverio-bt-350.

[69] Olimex EEG-SMT Website. 2020. URL: https://www.olimex.com/Products/EEG/OpenEEG/EEG-SMT/open-source-hardware.

[70] Raspberry Pi 3 Website. 2020. URL: https://www.raspberrypi.org/products/raspberry-pi-3-model-b/.